Automatic fused tungsten carbide detection in weld pool

Maik Rosenberger[1], Chen Zhang[1], Karsten Günther[2],
Jean Pierre Bergmann[2], Gunther Notni[1]

[1] Technische Universität Ilmenau, Department of Quality Assurance and Industrial Image Processing, Gustav-Kirchhoff-Platz 2, 98693 Ilmenau

[2] Technische Universität Ilmenau, Department of Production Technology, Gustav-Kirchhoff-Platz 2, 98693 Ilmenau

Abstract This paper represents an image-based tool for quantitative characterization of the dissolution behaviour of fused tungsten carbides (FTC) in weld pool. For the metallographical investigations with microscopic images, a method for automatic detection of hard phases is proposed to quantify the amount and distribution of FTCs in the matrix material. With this tool, the dependence of the hard phase characteristic on the welding parameters was investigated.

Keywords: metallography, welding process, image segmentation.

1 Introduction and motivation

In order to increase the wear resistance of tools underlying severe abrasive stresses (e.g. mining and oil drilling industry), fused tungsten carbides (FTC) embedded in a ductile Ni-base alloy become more and more important as hardfacing material. FTCs comprise an eutectoid morphology of mono-tungsten carbide (WC) and di-tungsten carbide (W_2C), whereby high cooling rates during the manufacturing process are necessary in order to stabilise both phases below 1300°C [1]. The benefit is a combination of high hardness and fracture toughness, exceeding the tribological properties of other commercial available hard phases [2].

Due to the manufacturing process, the weldability of FTC poses a challenge, as these hard phases have a strong liability to thermally induced dissolution reducing the wear performance of the hardfacing alloy [1,3–5]. In this context, the main reasons for the FTC degradation were not completely understood yet, so that several hypotheses currently exist referring to the high weld pool temperatures and dilution rates of the weld. Indeed, a deep understanding of the mechanisms is necessary in order to improve both welding process properties and hardfacing alloys [6–9].

In order to quantify the dissolution behaviour of FTC in dependence on the welding parameters, a software was developed, enabling a reliable detection of the hard phases in the cross section of the weld and thus giving a statement about the relation between the welding process parameters (welding feed speed, welding voltage and welding speed) and the content of the hard phases.

2 Experimental procedure

Dilution Rate A [%]

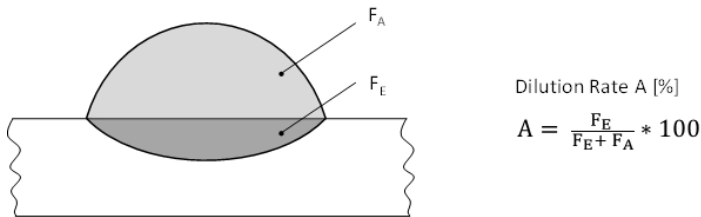$$A = \frac{F_E}{F_E + F_A} * 100$$

Figure 10.1: Definition of the dilution rate.

For metallographical investigations, three cross sections per sample were extracted at a weld seam length of 40, 50, 60 mm and finally grinded as well as polished in a multi-staged procedure. Macroscopically, the dilution rate A is of main interest, as defined in figure 10.1. The metallographically obtained contrast facilitated the detection of the hard phases by means of the developed program and hence a calculation of the percentage amount with respect to the weld surface ($F_E + F_A$).
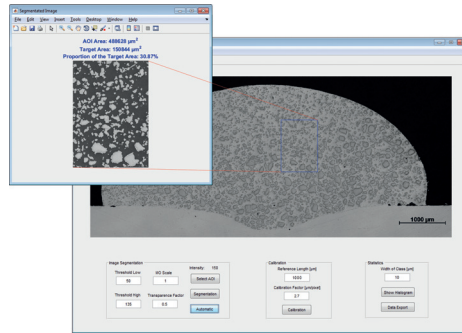
Figure 10.2: Detection of fused tungsten carbide (FTC) in the cross section of a hardfacing layer.

Through the calibration via the scale on the microscopic image, the calculated image resolution is 2.7 μm / pixel. The detection of the dark contrasted hard phases can be realized by adjusting the lower and upper threshold and thus localizing the relevant brightness intensity, see figure 10.2. Moreover, an algorithm for automatic hard phase detection is developed and will be extensively described in section 3.

Furthermore, the size distribution of the hard phases can be represented as histogram with user-defined class width, as shown in figure 10.3. The histogram offers another method for the characterisation of the microstructure of hard phases.

3 Automatic detection of hard phases

3.1 Evaluation of single methods

The hard phases are detected using image segmentation method. Generally, unsupervised methods for image segmentation could be divided into three classes: threshold-based, edge-based and region-based segmentation. In the first class, a set of threshold values is used to label different image regions and thus identifiy the target areas. A classical method for the automation of threshold selection is the Ostu's method [10], in which the optimal thresholds are determined by minimizing the within-class variance. The edge-based methods extract at first the outer contour of objects using different edge detectors [11].
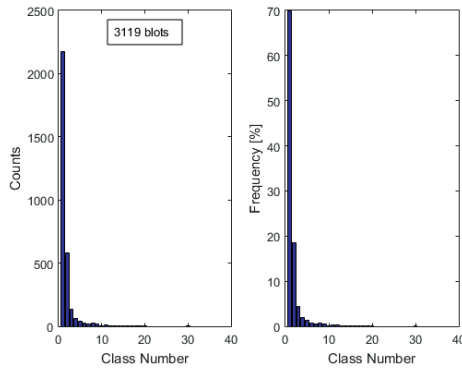
Figure 10.3: Histogram of hard phase sizes.

A considerable operator is the Canny detector for its ability in noise reduction and edge localization. Then, the small disconnectivities in the edges labeled by edge detectors must be eliminated so that closed region boundaries could be formed and identified as object regions. In the class of region-based methods, the active contour method is widely used. Starting from a set of initial object points, the neighboring pixels that satisfy a decision criterion are gradually added to the growing object region. As criterion, there is the region-based energy model [12] and the edge-based model [13]. The key step in the active contour method is a suitable selection of initial points to present the object property.

Besides these unsupervised methods, learning-based methods could be also used for image segmentation using support-vector-machine [14] or neural network [15]. But these methods need a high time expenditure for the collecting and labeling of training data. Therefore, only the unsupervised methods are taken into consideration within the framework of this work.

The challenge in the automation of hard phase detection is that the hard phases feature only a weak intensity contrast and the edge transition is irregular in part. With test images in grayscale, the Otsu's method, the Canny edge detector and active contour method are individually evaluated first of all. With the fact that the central areas of hard phase, the edge transition areas and the background build

approximately three classes, the Ostu's method is implemented with three levels. Furthermore, the resulting hard phase map is used as initial mask in the active contour method, in which the region-based energy model is used in order to overcome the irregularity of edge transition behavior.

To oppress the small-scale noise textures in background which could lead to false connections of separate hard phases, the Canny edge detector is implemented with increasing σ values and the resulting edge maps are pixelwise summed to generate an integral map. It is assumed that pixels with high integral indices refer to true edges, because the peak locations of small-scale edges become unreliable or disapperare with large σ values [16]. Then, the small fractures in the contours are removed with morphological bridge operator, and the hard phase areas are identified with hole filling operation.

From the results in figure 10.4, it can be seen that the Otsu's method can only achieve a coarse segmentation with much noise and plenty of false connections between large particle areas, probably due to the inhomogeneity of intensity distribution. In contrast, the Canny detector based method can realize a clean seperation of different particle areas, but some large particles are missed, because there are significant weak points on their contours that are not identified by the edge detector, so that closed boundaries cannot be builded at these areas.

Using the hard phase map obtained with the Otsu's method as initial mask, the active contour method achieves an improved segmentation result, as shown in figure 10.4 c. However, there remain still some noise and false connectivities. Therefore, an improved initial mask with less noise and false connectivites is needed to achieve a better segmentation result.

In section 3.2, a hybrid method will be described, which combines the aforementioned single methods into a complex procedure and could achieve an improved performance.

3.2 Proposed hybrid method

Figure 10.5 illustrates the proposed method that is based on the active contour method for the detection of hard phases. For the performance enhancement of the active contour method, the initial mask that is obtained with the Ostu's threshold is processed with erosion and opening
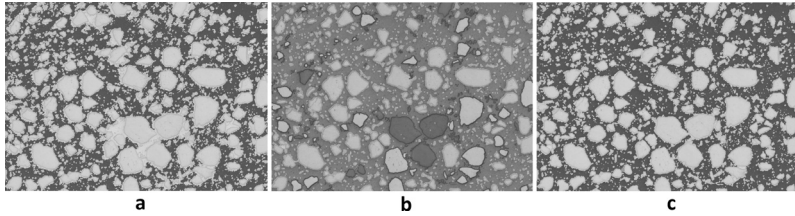
Figure 10.4: Hard phase detection based on different single methods. a: Otsu's threshold. b: Canny edge detector. c: active contour.

operation in order to disconnect independent hard phase areas clearly. But as a result, some small hard phase areas could disappear after these morphological operations. Therefore, the segmentation result with the active contour method is then merged with the hard phase map obtained with the Canny detector based method described in section 3.1, so that hard phases in all sizes can be accurately and cleanly extracted.
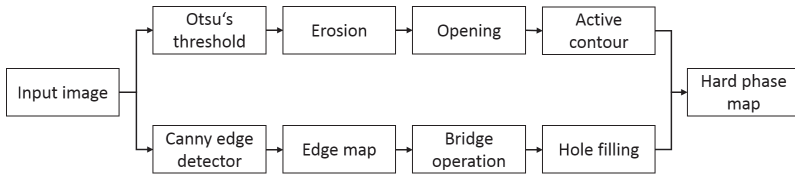

Figure 10.5: Proposed method for hard phase detection.

Figure 10.6 shows the segmented hard phase map with the proposed method. It is obvious that the boundaries of hard phase areas are extracted with high accuracy, and false connectivities can be avoided in principle.

4 Results and future work

Representative cross sections, see figure 10.7, illustrate the influence of the process parameters on the amount and distribution of FTCs in the Ni-base matrix material. It can be noticed, that an increase of the wire feed speed v_{GMAW} and welding voltage U_{GMAW} is going along
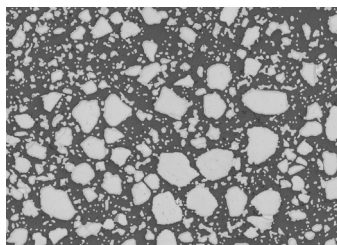
Figure 10.6: Detected hard phases with the proposed method.

with a rising dilution rate and a decrease of the hard phase content in the weld. However, metallographic investigations give only a qualitative statement concerning the relation between process parameters and microstructure.
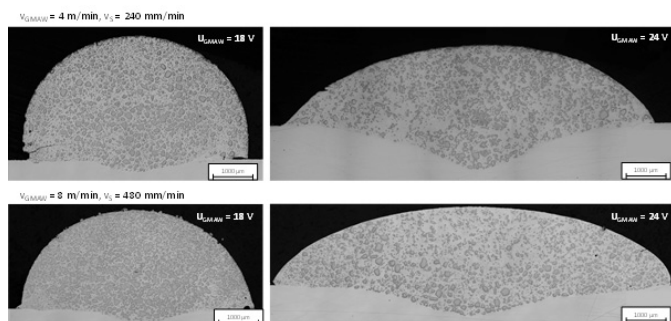

Figure 10.7: Influence of process parameters on the dilution and the hard phase characteristic.

Taking all investigated process parameters into account, the detection of the hard phase content finally evinced a dependency on the dilution rate, as depicted in figure 10.8. Maximum contents of app. 40 % at a dilution rate below 5 % could only be realized in between a narrow process window, including low wire feed speeds (v_{GMAW} = 4 m/min) and welding voltages U_{GMAW} (U_{GMAW} = 18 to 20 V). In return, a rising dilution rate of up to app. 40 % is synonymous with an almost complete extinction of FTC in the matrix.
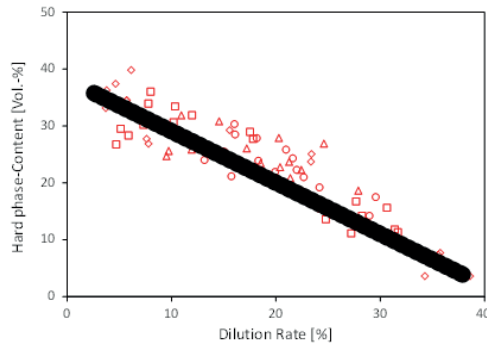
Figure 10.8: Relation between the hard phase content and the dilution rate.

Hence, by means of the developed software tool it could be proofed quantifiably, that the FTC dissolution shows a systematic dependency on the dilution to the substrate material (dilution rate), see figure 10.8. In contrast to the metallographic analysis, as shown in figure 10.7, this finding enables a specific adjustment of the welding process improving the wear performance of Ni-FTC hardfacings.

In the future, investigations based on histogram of hard phase size will be also performed to characterise the influences of welding parameters on the size distribution of hard phases.

References

1. F. Schreiber, *Wolfram-Schmelzkarbid im Verschleißschutz: Besonderheiten bei der schweißtechnischen Verarbeitung und Qualitätsicherung*.   Fachartikel der Durum Verschleißschutz GmbH, 2000.

2. H. Berns, *Hartlegierungen und Hartverbundwerkstoffe*.   Springer, 1998.

3. V. Z. Kublii and T. Y. Velikanova, "Ordering in the carbide W_2C and phase equilibria in the tungsten-carbon system in the region of its existence," in *Powder Metallurgy and Metal Ceramics*, vol. 43, pp. 630–644.

4. A. S. Kurlov and A. I. Gusev, "Tungsten carbides and W-C phase diagram," in *Inorganic Materials*, vol. 42, pp. 121–127.

5. R. Reiter, F. Schreiber, and K. Wernicke, "Verschleißeigenschaften von

Wolframkarbid-Hartlegierungen," in *Tagungsband zum 7. Werkstofftechnischen Kolloquium*, Chemnitz, Germany, 2004.

6. P. Vespa, P. T. Pinard, R. Gauvin, and M. Brochu, "Analysis of WC/Ni-based coatings deposited by controlled short-circuit MIG welding," in *Journal of Materials Engineering and Performance*, vol. 21, pp. 865–876.

7. E. Badisch and M. Kirchgassner, "Influence of welding parameters on microstructure and wear behaviour of a typical NiCrBSi hardfacing alloy reinforced with tungsten carbide," in *Surface and Coating Technology*, vol. 202, pp. 6016–6022.

8. L. Choi, M. Wolfe, M. Yarmurch, and A. Gerlich, "Effect of welding parameters on tungsten carbide-metal matrix composites produced by GMAW," in *Proceedings of Canadian Welding Association Conference*, Alberta, Canada, 2011.

9. L. J. Li and C. B. Gui, "Effect of dissolving of WC/W_2C on the interface microstructure of iron matrix hardfacing alloys," in *Advanced Materials Research*, vol. 306-307, 2011, p. 819–822.

10. N. Otsu, "A threshold selection method from gray-level histograms," in *Transactions on Systems, Man, and Cybernetics*, vol. 9, 1979, pp. 62–66.

11. D. Zhou and S. Tabbone, "Edge detection techniques: An overview," in *International Journal of Pattern Recognition and Image Analysis*, vol. 8, 1998, pp. 537–559.

12. V. Caselles, R. Kimmel, and G. Sapiro, "Geodesic active contours," in *International Journal of Computer Vision*, vol. 22, 1997, pp. 61–79.

13. T. F. Chan and L. A. Vese, "Active contours without edges," in *IEEE Transactions on Image Processing*, vol. 10, 2001, pp. 266–277.

14. J. Lu, D. Wang, L. Shi, and P. A. Heng, "Automatic liver segmentation in CT images based on support vector machine," in *Proceedings of theIEEE-EMBS International Conference on Biomedical and Health Informatics*, 2012, pp. 333–336.

15. M. Oquab, L. Bottou, I. Laptev, and J. Sivic, "Is object localizationfor free? -Weakly-supervised learning with convolutional neural networks," in *Proceedings of the IEEE Conference on Computer Vision and Pattern Recognition*, 2015, pp. 685–694.

16. X. Ren, "Multi-scale improves boundary detection in natural images," in *Proceedings of European Conference on Computer Vision 2008*, Marseille, France, 2008.